Determination of Relaxation and Retardation Spectrum from Modulus of Complex Frequency-Domain Material functions

VAIRIS SHTRAUSS, ALDIS KALPINSH
Institute of Polymer Mechanics
University of Latvia
23 Aizkraukles Street, LV 1006 Riga
LATVIA
strauss@edi.lv, kalpins@edi.lv

Abstract: - The paper is devoted to improving and simplifying determination of the relaxation and retardation spectrum (RRS). A concept is postulated that determination of RRS from some specially selected material responses differing from the explicitly defined material functions, such as the real or imaginary parts of complex compliance and complex modulus, may improve the recovery performance at the price of better measurability of these specific material responses. As one of possible implementations of the postulated concept, we propose to recover RRS from the modulus (absolute value) of a complex frequency-domain (dynamic) material function, which, compared to the real or imaginary part, can be more accurately and easy acquired by measuring the amplitudes of harmonic responses of a material. It is demonstrated that RRS recovery problem from the modulus of a complex frequency-domain material function may be interpreted as a filtering task with a *diffuse* magnitude response bounded by the responses of the Mellin deconvolution filters corresponding to the minimum (zero) and maximum imaginary parts according to the Kramers-Kronig relation. A discrete RRS recovery filter operating with geometrically sampled data is constructed for recovering RRS from the modulus and the simulation results are presented. A measurement system is proposed implementing RRS recovery through the modulus of a complex frequency-domain material function, where a material under test is subjected to multi-harmonic excitation at geometrically spaced frequencies with subsequent measuring the amplitudes of multi-harmonic responses and processing them by a discrete RRS recovery filter.

Key-Words: - Relaxation and Retardation Spectrum (RRS), Modulus of a Complex Frequency-Domain Function, Complex Compliance, Complex Modulus, Mellin Deconvolution Filter, Diffuse Magnitude Response

1 Introduction

Relaxation and retardation spectrum (RRS) is one of the most fundamental quantities in linear theory of viscoelasticity [1-4] and other relaxation theories [4-6]. RRS relates to molecular structure of materials [7-9], it is independent of loading (excitation) and is used in various studies, such as examination of the relationship between the molecular weight distribution and properties of a material, prediction of the behaviour of materials after an arbitrary excitation, interconversion of material functions, etc.

Traditionally, RRS is determined from various experimental time-domain (static) or frequency-domain (dynamic) material functions, which go by different names in specific experiments [1-6]. However, in the most cases, these functions represent the characteristic responses of a material to the three standard excitations (loadings) [10], such as step (the Heaviside step function), impulse (the Dirac delta function) and harmonic (the steady-state sinusoidal) ones, and may be generalized into two categories as *modulus functions* in the case of the *displacement* (strain, charge, etc.) excitation and *compliance functions* in case of the *force* (stress, voltage, etc.) excitation.

In its turn, approaches used for RRS determination can be classified as *parametric* and *non-parametric* ones [11,12]. The parametric approach presumes an *a priori* model form for the material behaviour and RRS is determined based on parametric curve fitting techniques. Contrary, no any assumption made about the material behaviour for the non-parametric approach, where RRS is determined by numerical inversion of the integral transforms, which interconnect the material responses with the spectrum. These inversions are known to be fundamentally ill-posed in the sense that small perturbations in the input data can yield unrealistic high perturbations in the spectra.

Despite that the performance of RRS recovery, particularly for non-parametric methods, depends on both the experimental stage (input data acquisition) and on the data processing stage (RRS recovery), determination of RRS is generally considered only as

a one-stage operation of construction of a recovery algorithm from the explicitly defined material functions.

Since no processing result is better than the input data behind it, we postulate a concept that determination of RRS from some specially selected material responses differing from traditionally used material functions may improve the performance of RRS recovery at the price of the better measurability of these specific material responses. Accomplishment of this concept requires integration of the experimental and data processing stages, and actually leads to development of RRS measurement systems [10]. Usage of optimised excitations may be a promising direction for improvement RRS recovery in the light of the postulated concept.

In presented paper, as one of possible implementations of the proposed concept, we consider the determination of RRS from the *modulus* (absolute value)[1] of complex frequency-domain material functions, which, compared to the real or imaginary parts, can be more accurately acquired by measuring the amplitudes of responses of a material to the harmonic excitations [13].

2 Theoretical Background

If a material under test (MUT) is subjected to harmonic steady-state excitation with amplitude X_m

$$x_m(t) = X_m \sin \omega_m t, \tag{1}$$

it responds by a harmonic response of the same frequency ω_m but with a different amplitude and phase

$$y_m(t) = Y_m \sin(\omega_m t - \varphi_m), \tag{2}$$

where Y_m is amplitude and φ_m is phase angle of the response with respect to the excitation.

Amplitude Y_m is proportional to the modulus of a complex frequency-domain material function at frequency ω_m. Thus, for a MUT with *complex modulus* $\tilde{G}(\omega) = G'(\omega) + jG''(\omega)$, where $G'(\omega)$ is the real part (storage modulus), $G''(\omega)$ is the imaginary part (loss modulus), and $j = \sqrt{-1}$, the amplitudes of the harmonic excitation and response are related as

$$\frac{Y_m}{X_m} = |\tilde{G}(\omega_m)| = \sqrt{[G'(\omega_m)]^2 + [G''(\omega_m)]^2}. \tag{3}$$

Likewise, in the case of a MUT with *complex compliance* $\tilde{J}(\omega) = J'(\omega) - jJ''(\omega)$, the amplitudes are described by expression similar to that of (3)

$$\frac{Y_m}{X_m} = |\tilde{J}(\omega_m)| = \sqrt{[J'(\omega_m)]^2 + [J''(\omega_m)]^2}, \tag{4}$$

where $J'(\omega)$ and $J''(\omega)$ are the real part (storage compliance) and the imaginary part (loss compliance), respectively.

According to the linear relaxation theories [1-6], the real and imaginary parts of complex modulus are related to RRS by the following integral transforms:

$$G'(\omega) = G_0 + \int_0^\infty \frac{F(\tau)\omega^2\tau^2 d\tau}{1+\omega^2\tau^2}, \tag{5}$$

$$G''(\omega) = \int_0^\infty \frac{F(\tau)\omega\tau\, d\tau}{1+\omega^2\tau^2}, \tag{6}$$

where $F(\tau)$ is *relaxation spectrum* named also *function of distribution of relaxation times*, and G_0 is so-called static modulus observed for $G'(\omega)$ at zero frequency.

Similarly, the following expressions are valid for the real and imaginary parts of complex compliance

$$J'(\omega) = J_\infty + \int_0^\infty \frac{F(\tau)d\tau}{1+\omega^2\tau^2}, \tag{7}$$

$$J''(\omega) = \int_0^\infty \frac{F(\tau)\omega\tau\, d\tau}{1+\omega^2\tau^2}. \tag{8}$$

In this case, $F(\tau)$ is *retardation spectrum* named also *function of distribution of retardation times*, and J_∞ represents so-called instantaneous component of compliance observed for $J'(\omega)$ at infinite frequency.

A large number of methods [11,12,14-18] based on different ideas have been proposed for inversion of integral transforms (5) – (8). We have developed a computationally efficient *functional filtering approach* [19-22] for executing a wide variety of interconversions between viscoelastic material functions, including the ones between the time-domain and frequency-domain functions, and vice versa [23], the interconversion between the real and imaginary part of frequency-domain functions [24], as well as calculation of RRS [25,26]. The functional filtering approach has well grounded basis on the advanced signal processing [27] and the

[1] The modulus (absolute value) of a complex frequency-domain function may not be confused with *modulus function* representing the response of a material to *displacement excitation.*

interconversions are executed by discrete Mellin convolution or deconvolution filters operating with geometrically sampled data.

3 Functional Filtering Approach

3.1 Underlying Idea

The central idea behind the functional filtering approach is based on the following two key points:

(i) functions of materials exhibiting relaxational behaviour behave monotonically or locally monotonically and so are experimentally recorded over many decades of time or frequency. For this reason, the widely used practice [1-6] is to consider these functions on a logarithmic time or frequency scale;

(ii) interrelations between various material functions, including these with RRS, are described by the integral transforms having kernels depending on the ratio or product of arguments. For example, integral transforms (5) – (8) are ones with kernels depending on product $\omega\tau$.

The mentioned transforms can be converted in the form of the Mellin convolutions

$$y(u) = x(u) \overset{M}{*} k(u) = \int_0^\infty x(r) k\left(\frac{u}{r}\right) \frac{dr}{r} \tag{9}$$

for direct transforms, and

$$x(u) = y(u) \overset{M}{*} k(u) = \int_0^\infty y(r) k\left(\frac{u}{r}\right) \frac{dr}{r} \tag{10}$$

for inverse transforms, where $x(u)$ is some experimental (recorded) material function (input function), $y(u)$ is some unknown function to be determined (output function), $\overset{M}{*}$ denotes the Mellin convolution, and $k(u)$ is a kernel depending on the ratio of arguments u/r, which will be named further *Mellin kernel*.

For logarithmic variables, Mellin convolution type transforms (9) and (10) alter into the Fourier convolution type transforms. Since Fourier convolution type transforms describe *linear shift-invariant systems* or *linear filters* [27], the interrelations between material functions with kernels depending on the ratio or product of arguments may be interpreted as *ideal filters* operating on a logarithmic time or frequency scale. This builds a theoretical foundation for executing the interconversions between material functions by discrete and digital filtering techniques approximating ideal systems (9) and (10). Since uniformly sampled data on the logarithmic time or frequency scale manifest as the samples distributed according to geometric progression in the linear scale, functional filters operate with data at geometrically spaced times or frequencies.

The functional filtering approach has several advantages. Digital filters are computationally efficient algorithms working without employing numerical integration [27]. Algorithms for the interconversions between material functions are constructed with uniform structure and implementation in software and hardware. Various interconversion problems are modified very easy by changing filter coefficients without modification of the common structure or implementation of the algorithm in hardware and software. For correctly designed digital filters no stability problems occur and they have the guaranteed performance, such as accuracy and sensitivity to noise.

3.2 Functional Filters for RRS recovery

In general, determination of RRS relates to inversion of Eq. (10). The algorithms for RRS recovery from the real and imaginary parts of a frequency-domain function have been derived in the form [25,26]:

$$F(u_0 q^m) = \begin{cases} \sum_{n=-(N-1)/2}^{(N-1)/2} h[n] x\left(q^{-n-m}/u_0\right) \text{for an odd } N \\ \sum_{n=-(N-2)/2-1}^{(N-2)/2} h[n] x\left(q^{-0.5-n-m}/u_0\right) \text{for an even } N \end{cases} \tag{11}$$

where $h[n]$ is impulse response containing N non-zero filter coefficients, $x(.)$ represents the real ($G'(\omega)$, $J'(\omega)$) or imaginary ($G''(\omega)$, $J''(\omega)$) parts, q is progression ratio specifying the sampling rate in the sense that $\ln q$ defines the distance between samples on the logarithmic frequency scale, i.e. plays formally a role of sampling period, whereas its reciprocal describes the appropriate sampling frequency, and u_0 is an arbitrary normalization constant usually chosen to be equal to 1.

By making substitution $\tau = u_0 q^m$, algorithms (11) may be simplified

$$F(\tau) = \begin{cases} \sum_{n=-(N-1)/2}^{(N-1)/2} h[n] x\left(q^{-n}/\tau\right) \text{for an odd } N \\ \sum_{n=-(N-2)/2-1}^{(N-2)/2} h[n] x\left(q^{-0.5-n}/\tau\right) \text{for an even } N \end{cases}. \tag{12}$$

Filters (11) and (12) have periodic frequency responses in the Mellin transform domain

$$H(e^{j\mu}) = \sum_n h[n]\exp(-j\mu n \ln q), \quad (13)$$

which within main period $[-\pi/\ln q, \pi/\ln q]$, named *filter bandwidth*, approximates non-periodic frequency responses

$$H(j\mu) = M[k(u);-j\mu] = \int_0^\infty k(u)u^{-j\mu-1}du \quad (14)$$

of ideal direct filters executing transforms (9), and

$$H(j\mu) = 1/M[k(u);-j\mu] = 1/\int_0^\infty k(u)u^{-j\mu-1}du \quad (15)$$

of ideal inverse filters inverting transforms (10). In Eqs. (14) and (15), M denotes the Mellin transform [28], parameter μ, named *Mellin frequency*, is interpreted [22,25,26] as the angular frequency for a function on the logarithmic time or frequency scale, and summation index n in Eq. (13) depending on evenness or oddness of N runs in accordance with Eq. (11) or (12).

3.3 Regularization via Sampling Rate

It is well known that determination of RRS is a fundamentally ill-posed problem [29] needed that special stabilization or regularization procedures are used to minimize the sensitivity to noise. Different regularization methods have been proposed [14-16]. However, irrespective of the idea and complexity of a particular regularization method, stabilization for all the methods is attained at the expense of accuracy.

As it is shown [30,31], the ill-posedness for linear inverse problems, i.e. inverse functional filters comes from their increasing magnitude responses $|H(j\mu)|$ (Fig. 1(a)) causing that noise amplification coefficients of the appropriate discrete filters

$$S = \sum_n h^2[n] \quad (16)$$

may take the values much greater than 1. Since noise amplification coefficient (16) multiplies variance σ_x^2 of input noise (random error) to give noise variance σ_y^2 of an output function

$$\sigma_y^2 = S\sigma_x^2,$$

the filter becomes sensitive to input noise in the case when $S >> 1$.

According to the Parseval's relation [27], the noise amplification coefficient can be also determined by square integration of the magnitude response of a filter

$$S = \ln q/(2\pi)\int_{-\pi/\ln q}^{\pi/\ln q} |H(j\mu)|^2 d\mu. \quad (17)$$

From Eq. (17), it follows that, for increasing magnitude responses (see Fig. 1(a)), extension of filter bandwidth $[-\pi/\ln q, \pi/\ln q]$ by a decrease of progression ratio q enlarges the area (shaded region) under the increasing magnitude response and, due to squared integration of the increasing magnitude response, causes that the noise amplification coefficient tends to infinity ($S \to \infty$) when $\ln q \to 0$ or $q \to 1$ (Fig. 1(b)). Therefore, depending on q, inversion problem can be well- or ill-conditioned, or, in other words, progression ratio q, or the sampling rate in general, may be used for controlling noise amplification of inverse filters, i.e. for their regularization.

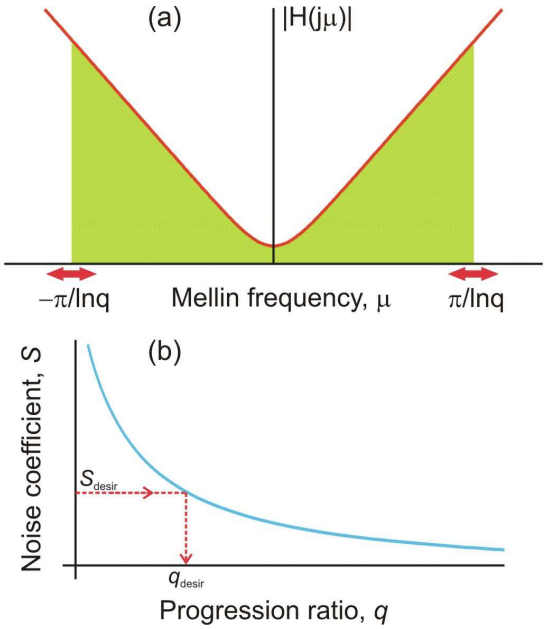

Fig. 1. Increasing magnitude response (a) and noise amplification coefficient versus progression ratio (b) for an inverse filter.

The appropriate regularization procedure [32, 33] has been developed, which, for available (limited) frequency range of input data, searches a combination of progression ratio q and a number of filter coefficients N providing bandwidth $[-\pi/\ln q, \pi/\ln q]$, which ensures desired – previously specified – noise amplification coefficient S_{desir} (see Fig 1(b)). Contrary to other regularization methods [14-16,29], where noise amplification for linear problems is typically minimized by limiting (in the filtering light – distorting) increasing magnitude responses at high frequencies, in the proposed

regularization, the desired noise amplification is attained by eventual violation of the sampling theorem [27], i.e. at the expense of decreased accuracy due to the eventual aliasing effects. The superiority of the proposed method is that it is very simple and so computationally efficient. Actually, no special denoising takes place for an inverse filter in this case. The filter is simply enforced to operate at sufficient low sampling rate (sufficient large progression ratio q_{desir}), which guarantees the desired noise amplification (see Fig 1(b)). The second advantage of the method is its transparency, it allows explicit determination of regularization parameter – progression ratio q_{desir} [32,33] at which desired noise amplification coefficient S_{desir} is attained, while there no strong criterion for determination of regularization parameters for the traditional regularization methods leading that human involvement is necessary to set appropriate regularization parameters.

3.4 Design of Functional Filters

Design problem of a RRS recovery filter can be formulated as finding filter coefficients $h[n]$, which for available or given frequency ranges of input data generates maximum accurate spectrum waveforms with acceptably low noise amplification. A method for designing the functional filters – named *identification method* – has been developed [19,25] based on system identification and learning principles. The block-diagram the identification method is shown in Fig. 2. Contrary to conventional design methods of digital filters [27], the identification method implements filter design in the *input-output function domain*. A pair of exact (theoretical) functions interrelated to each other by an integral transform to be performed are used input and output ones in the identification process. The method implements so-called grey-box modelling, when structure of the algorithm to be constructed (progression ratio q, number of coefficients N, symmetry of coefficients, etc.) is assumed known and values of the coefficients are determined by minimizing the error between an exact output function and that obtained by filtering.

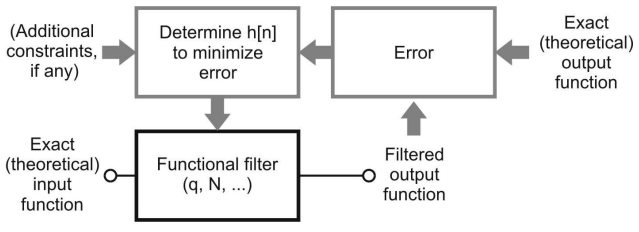

Fig. 2. Block-diagram of the identification method.

An advantage of the identification method is that it effectively disposes of various secondary effects such as data truncation, rounding-off, etc. and allows designing filters of various types, e.g. with and without symmetry of the coefficients, etc. Additional constraints, such as maximum acceptable noise amplification coefficient, can easily be imposed on the solution to ensure special targets.

4 Recovery of RRS from the Modulus of Frequency-Domain Functions

Due to the operations of rising to the power and taking square root in Eqs. (3) and (4), the interrelation between the modulus and RRS cannot be written in the terms of a Mellin convolution and, consequently, the RRS recovery problem from the modulus cannot be formally formulated as a functional filtering task.

4.1 Limiting Cases for the Modulus

Since the real and imaginary parts of causal physical systems, such as materials are not wholly independent but are linked by the Kramers-Kronig relations [24,34], two limiting cases can be defined for modulus (3) and (4), when:

(i) the imaginary parts tend to zero

$$\left.\begin{matrix} G''(\omega) \\ J''(\omega) \end{matrix}\right\} \to 0,$$

then the modulus approaches to the appropriate real part

$$|\tilde{G}(\omega)| \to G'(\omega) \text{ and } |\tilde{J}(\omega)| \to J'(\omega), \tag{18}$$

and

(ii) the imaginary parts take maximum values according to the Kramers-Kronig relation

$$G''(\omega) = \frac{\omega\tau}{1+\omega^2\tau^2}, \text{ then } G'(\omega) = \frac{\omega^2\tau^2}{1+\omega^2\tau^2},$$

and

$$|\tilde{G}(\omega)| = \frac{\sqrt{\left(\frac{\omega^2\tau^2}{1+\omega^2\tau^2}\right)^2 + \left(\frac{\omega\tau}{1+\omega^2\tau^2}\right)^2}}{\frac{\omega\tau}{\sqrt{1+\omega^2\tau^2}}} = \tag{19}$$

for $G_0 = 0$, and

$$J''(\omega)=\frac{\omega\tau}{1+\omega^2\tau^2},\ \text{then}\ \ J'(\omega)=\frac{1}{1+\omega^2\tau^2},$$

and

$$|\tilde{J}(\omega)|=\sqrt{\left(\frac{1}{1+\omega^2\tau^2}\right)^2+\left(\frac{\omega\tau}{1+\omega^2\tau^2}\right)^2}=\frac{1}{\sqrt{1+\omega^2\tau^2}} \qquad (20)$$

for $J_\infty=0$.

Cases (18) are associated with very broad RRS, whereas RRS is equal to the line or the Dirac delta function in cases (19) and (20). For example, in Fig. 3, modulus (20) and real part (7) of complex compliance are shown corresponding to the Cole-Cole (CC) relaxation response [35] for different values of spectrum parameter α. As it is seen, a relatively large difference between the modulus and the real part is observed for $\alpha=1$ (the Dirac delta function spectrum), and it gradually decreases for smaller value of α (broader spectra).

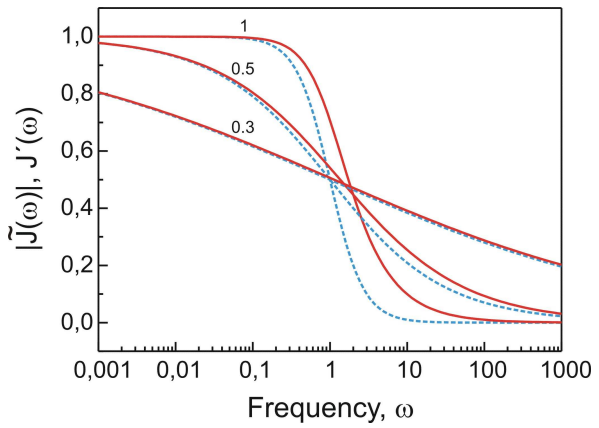

Fig. 3. The modulus (solid) and real parts (dashed) of complex compliance corresponding to CC relaxation model at different values of parameter α (numbers near the curves).

From limiting cases (18), it follows that determination of RRS from the modulus for materials with the small imaginary parts leads to the ideal Mellin deconvolution filters recovering relaxation spectrum from the real parts having the following frequency responses [25,26]

$$H(j\mu)=\pm\frac{2}{\pi}\sin\frac{j\pi\mu}{2}=\pm j\frac{2}{\pi}\mathrm{sh}\frac{\pi\mu}{2}, \qquad (21)$$

where $H(j\mu)$ with plus sign relates to the filter for determination of the spectrum from $J'(\omega)$, while $H(j\mu)$ with minus sign – to the filter for determination of the spectrum from $G'(\omega)$.

For materials with the large imaginary parts, limiting cases (19) and (20) can be also generalized as Mellin convolutions. Thus, interrelation between $|\tilde{G}(\omega)|$ and $F(\tau)$ for limiting case (19) can be described by the following Mellin convolution type transform

$$|\tilde{G}(\omega)|=\int_0^\infty\frac{F(1/\tau)\omega/\tau}{\sqrt{1+\omega^2/\tau^2}}\frac{d\tau}{\tau} \qquad (22)$$

with Mellin kernel $k(u)=u/\sqrt{1+u^2}$. According to Eq. (15), inversion of (22) leads to an ideal Mellin deconvolution filter with the frequency response

$$H(j\mu)=1/\int_0^\infty\frac{u^{-j\mu}}{\sqrt{1+u^2}}du=\frac{2\sqrt{\pi}}{\Gamma(-1/2-j\mu/2)\Gamma(1+j\mu/2)}, \qquad (23)$$

where Γ is the Gamma function.

Similarly, for complex compliance $\tilde{J}(\omega)$, limiting case (20) can be generalized in the form of the following Mellin convolution type transform

$$|\tilde{J}(\omega)|=\int_0^\infty\frac{F(1/\tau)}{\sqrt{1+\omega^2/\tau^2}}\frac{d\tau}{\tau} \qquad (24)$$

with kernel $k(u)=1/\sqrt{1+u^2}$. Inversion of Eq. (24) leads to the ideal Mellin deconvolution filter with frequency response

$$H(j\mu)=1/\int_0^\infty\frac{u^{-j\mu-1}}{\sqrt{1+u^2}}du=\frac{2\sqrt{\pi}}{\Gamma(-j\mu/2)\Gamma(1/2+j\mu/2)}. \qquad (25)$$

4.2 Diffuse Magnitude Response

Frequency responses (21) of the limiting filters for determining RRS from the real parts of complex modulus and complex compliance differ by signs and so have equal magnitude responses $|H(j\mu)|$. Frequency responses (23) and (25) of the limiting filters for the large imaginary parts of complex modulus and complex compliance also have equal magnitude responses. The equality of these magnitude responses follows from the fact that the Mellin kernels for integral transform (22) interrelating $|\tilde{G}(\omega)|$ with $F(\tau)$, and integral

transform (24) interrelating $|\tilde{J}(\omega)|$ with $F(\tau)$, differ by multiplier u

$$k_{\text{mod}}(u) = uk_{compl}(u),$$

resulting that their Mellin transforms are the shifted functions of one other [28]

$$H_{\text{mod}}(j\mu) = H_{compl}(j\mu + 1)$$

related as

$$H_{\text{mod}}(j\mu) = H_{compl}(j\mu)e^{j\mu}$$

with equal absolute values $\left|H_{\text{mod}}(j\mu)\right| = \left|H_{compl}(j\mu)\right|$.

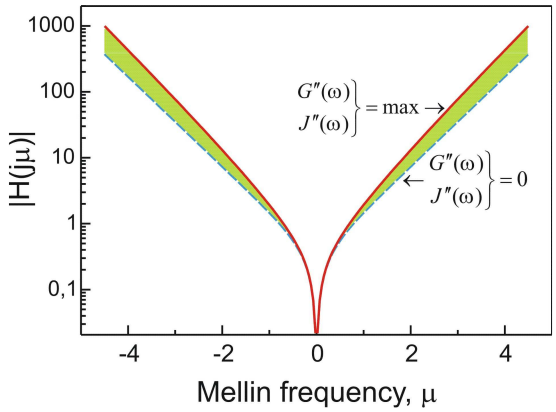

Fig. 4. *Diffuse* magnitude response (shaded area) bounded by limiting response of (21) (dashed) and a pair of magnitude responses of (23) and (25) (solid).

In Fig. 4, the magnitude responses are shown for the limiting filters corresponding to the minimum (zero) and the maximum imaginary parts. As it is seen, they are similar – extremely rapidly increasing functions located relatively close one another. It can assume that the ideal magnitude responses for all other cases of determination of RRS from the modulus should lie in the lane between the both responses (shaded area). Therefore, the problem of determination of RRS from the modulus of frequency-domain material functions may be interpreted as a functional filtering task with a *diffuse* magnitude response bounded by the magnitude response for (21) and the magnitude response for (23) or (25). A practical conclusion follows that, despite that the interrelations between the modulus of frequency-domain material functions and RRS are no longer a Mellin convolution, RRS likely can be recovered from the modulus by the appropriate discrete inverse functional filters.

4.3 RRS Recovery Filters from the Modulus

RRS from the modulus of a frequency-domain material function is calculated by the same algorithms (11) and (12) used for the real and imaginary parts.

According to the symmetry properties of the Fourier transform [27], pure imaginary frequency response (21) enforces an odd symmetry on impulse response $h[n]$ of the filters recovering RRS from the real parts [25]. Contrary to this, responses (23) and (25) are complex functions of μ, which do not predict any symmetry for $h[n]$ of the filters for RRS recovery from the modulus of a frequency-domain material function.

Since all frequency responses (21), (23) and (25) have zero values at zero Mellin frequency ($H(j0) = 0$) (see Fig. 4), the filters cut out zero frequency (DC) component of an input function. This means that the RRS recovery filters are insensitive to bias or bias-invariant of an input function, which is very important for practice, because no special measure to be taken to separate components G_0 and J_∞ from the whole response functions to obtain their relaxing parts.

Table 1. Coefficients $h[n]$ for 6-point filters designed for recovering the retardation spectrum from the modulus (filter 1) and from the real part (filter 2)

n	Filter 1	Filter 2
-3	0.002118	-0.0621334
-2	0.212985	0.577504
-1	-1.49284	-2.25364
0	1.53843	2.25364
1	-0.271549	-0.577504
2	0.0108601	0.0621334

Relatively similar magnitude responses of the filters recovering RRS from the modulus of a frequency-domain material function to those recovering RRS from the real parts (see Fig. 4) allows to use approximately the same filter specification (q and N) to ensure the desired performance (accuracy and noise amplification). Thus, the specification with $q = 3.3$ and $N = 6$ proposed in [25,26] has been chosen, which should ensure noise amplification coefficient (16) of the order of 10. For the mentioned specification, algorithm (12) takes the form:

$$F(\tau) = \sum_{n=-3}^{2} h[n]x(3.3^{-0.5-n}/\tau). \qquad (26)$$

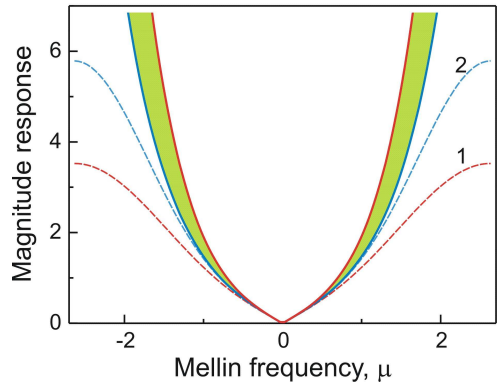

Fig. 5. Magnitude responses of filters 1 and 2. Shaded area: ideal *diffuse* magnitude response.

Coefficients $h[n]$ for (26) for recovering the retardation spectrum from the modulus of complex compliance are given in Table 1 (filter 1), which according to Eq. (16) ensure actual experimental noise amplification coefficient $S = 4.72$. For comparison, the coefficients are also presented in Table 1 for a 6-point filter recovering the retardation spectrum from the real part [25,26] having $S = 10.83$ (filter 2). Fig. 5 illustrates the magnitude responses of the both recovery filters.

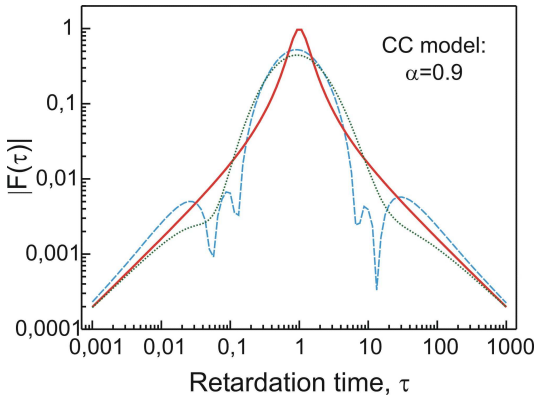

Fig. 6. Retardation spectrum for CC model at $\alpha = 0.9$ recovered from the modulus by filters 1 (dotted) and 2 (dashed). Solid line: exact spectrum.

4.4 Simulation Results

The simulations performed have demonstrated that, for the narrow spectra ($\alpha > 0.8$), the better results give the filters designed for spectrum recovering from the modulus, i.e. these be constructed for inverting Eq. (24). However, for the broader spectra, the accuracy of the filters designed for spectrum recovering from the modulus and the real part is approximately the same.

As an example, in Fig. 6 and 7, the retardation spectrum corresponding to CC relaxation model [35] with $J_\infty = 2$, and $\alpha = 0.9$ and $\alpha = 0.8$ are shown recovered from noiseless input data by filter 1 and filter 2. If filter 2 designed for recovering spectrum from the real part gives an oscillating spectrum at $\alpha = 0.9$, then already at $\alpha = 0.8$, the recovery results are very similar for the both filters.

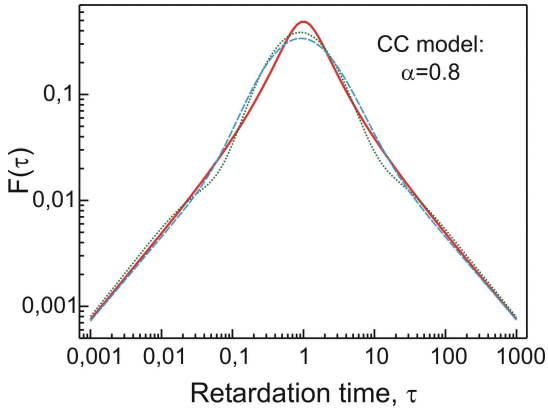

Fig. 7. Retardation spectrum for CC model at $\alpha = 0.8$ recovered from the modulus by filters 1 (dotted) and 2 (dashed). Solid line: exact spectrum.

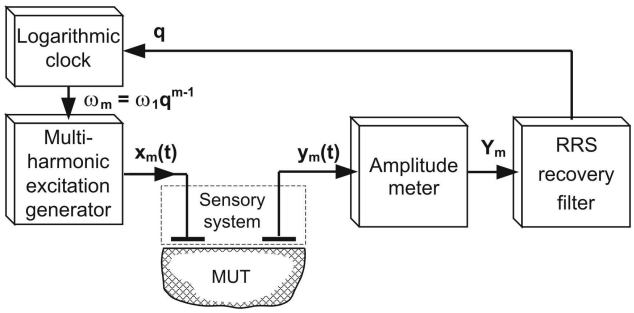

Fig. 8. Block diagram of a measurement system implementing RRS recovery through the modulus of a complex frequency-domain function.

5. RRS Measurement System

Determination of RRS from the modulus of a complex frequency-domain material function gives a basis for simplifying RRS measurement system [10]. If classical approach of determination of the real or imaginary part of a complex frequency-domain material function requires such operations as (i) measurement of amplitudes of harmonic excitations, (ii) measurement of amplitudes of responses, (iii) measurement of phase differences between the excitations and responses, and (iv) calculation of the real or imaginary part, determination of the modulus according to Eqs. (3) and (4) leads to measurement of harmonic amplitudes only. However, the basic impact on improving the performance of RRS

recovery comes from the potentially increased accuracy of measurement of the amplitudes compared to the accuracy of measurement of the real part and, particularly, of the imaginary part.

For implementation of RRS recovery through the modulus of a complex frequency-domain function, we propose to develop a RRS measurement system [13], which executes an active measurement experiment by exciting MUT with multi-harmonic excitations, measuring MUT responses and processing them by a RRS recovery filter. A general block diagram of the system is shown in Fig. 8.

A harmonic electrical excitation signals $x_{\mathrm{m}}(t)$ from a *multi-harmonic excitation generator* at geometrically spaced frequencies ω_{m}

$$\omega_m = \omega_1 q^{m-1} \tag{27}$$

are transmitted to a *sensory system*, which produces appropriate physical (mechanical, electrical, magnetic, thermal, etc.) excitations to MUT and detects and converts MUT responses back into electrical signals $y_{\mathrm{m}}(t)$. The amplitudes of these electrical response signals are measured by an *amplitude meter*. To calculate RRS, the measured amplitudes are processed by a *RRS recovery filter*. To provide the geometrically spaced frequencies, the multi-harmonic excitation generator is controlled by a *logarithmic clock* generating logarithmic clock signals for reference frequencies (27).

6 Conclusions

A concept is postulated that determination of RRS from certain material responses differing from the explicitly defined material functions, such as the real or imaginary parts of complex compliance and complex modulus, may improve the recovery performance of RRS at the price of the better measurability of these specific responses. As one of possible implementations of the postulated concept, it is proposed to recover RRS through the modulus (absolute value) of a complex frequency-domain (dynamic) material function, which, compared to its real or imaginary part, can be more accurately acquired by measuring amplitudes of the harmonic responses of a material.

The problem of determination of RRS from the modulus is analysed and solved based on the functional filtering approach. While the problem cannot be represented in the terms of a Mellin convolution due to the operations of rising to the power and taking the square root necessary for defining the modulus, it formally cannot be formulated as a functional filtering task. However, two limiting cases for the modulus – corresponding to the small (zero) and the large (maximum) imaginary parts – can be represented in the form of the Mellin convolution, from which it follows that two ideal limiting Mellin deconvolution filters can be derived for these cases. Based on this, the problem of determination of RRS from the modulus of a complex frequency-domain material function is formulated as a functional filtering task with a *diffuse* magnitude response bounded by the magnitude responses of the two limiting deconvolution filters.

A discrete RRS recovery filter operating with geometrically sampled data is designed for recovering RRS from the modulus and the simulation results are presented. It is shown that the filters designed for RRS recovery from the real parts are also applicable for recovering RRS from the modulus, particularly, for the broader spectra. For the narrower spectra, however, the better results give the algorithms designed for recovering the spectrum from the modulus.

A measurement system is proposed implementing RRS recovery through the modulus of a complex frequency-domain material function, where a material under test is subjected to multi-harmonic excitations at geometrically spaced frequencies, and amplitudes of multi-harmonic responses are measured and processed by a RRS recovery filter.

Acknowledgements

This work was supported by the European Regional Development Fund (ERDF) under project No. 2010/0213/2DP/2.1.1.1.0/10/APIA/VIAA/017.

References:

[1] J.D. Ferry, *Viscoelastic Properties of Polymers*, 3rd. ed., J. Wiley and Sons, 1980.

[2] N.W. Tschoegl, *The Phenomenological Theory of Linear Viscoelastic Behavior;* Springer-Verlag, 1989.

[3] N.G. McCrum, B.E. Read, G. Wiliams, *Anelastic and Dielectric Effects in Polymer Solids*, J. Wiley and Sons, 1967.

[4] A.K. Jonscher, *Dielectric Relaxation in Solids*, Chelsea Dielectric, 1983.

[5] F. Kremer, A. Schonhals, W. Luck, *Broadband Dielectric Spectroscopy*; Springer-Verlag, 2002.

[6] C.P. Slichter, *Principles of Magnetic Resonance;* 3rd. enlarged and updated ed., Springer-Verlag, 1996.

[7] C. Friedrich, R.J. Loy, R.S. Anderssen, Relaxation time spectrum molecular weight

distribution relationships, *Rheol. Acta*, Vol. 48, 2009, pp. 151-162.

[8] M.R. Nobile, F. Cocchini, A general relation between MWD and relaxation time spectrum, *Rheol. Acta*, Vol. 47, 2008, pp. 509–519.

[9] W. Thimm, C. Friedrich, M. Marth, J. Honerkamp, An analytical relation between relaxation time spectrum and molecular weight distribution, *J. Rheol.*, Vol. 43, 1999, pp. 1663–1672.

[10] A. Kalpinsh, V. Shtrauss, Measurement systems for distribution of relaxation and retardation times, *Proc. 15th WSEAS International Conference on Systems RECENT RESEARCHES in SYSTEM SCIENCE*, Corfu Island, Greece, July 14-16, 2011, pp. 106-111.

[11] J.R. Macdonald, Comparison of parametric and nonparametric methods for the analysis and inversion of immittance data: Critique of earlier work, *J. Comp. Phys.*, Vol. 157, 2000, pp. 280-301.

[12] J.R. Macdonald, E. Tuncer, Deconvolution of immittance data: Some old and new methods, *J. Electroanalytical Chem.* Vol. 602, 2007, pp. 255-262.

[13] V. Shtrauss, A. Kalpinsh, Recovery of distribution of relaxation and retardation times by measuring amplitudes to multi-harmonic excitations, *Proc. 15th WSEAS International Conference on Systems RECENT RESEARCHES in SYSTEM SCIENCE*, Corfu Island, Greece, July 14-16, 2011, pp. 112-117.

[14] J. Honerkamp, J. Weese, Determination of the relaxation spectrum by a regularization method, *Macromolecules*, Vol. 22, 1989, pp. 4372–4377.

[15] C. Elster, J. Honerkamp, J. Weese, Using regularization methods for the determination of relaxation and retardation spectra of polymeric liquids, *Rheol. Acta*, Vol. 31, 1992, pp. 161-174.

[16] J. Honerkamp, J. Weese, A nonlinear regularization method for the calculation of relaxation spectra, *Rheol. Acta*, Vol. 32, 1993, pp. 65–73.

[17] F. Aslani, L. Sjögren, Relaxation rate distribution from frequency or time dependent data, *Chem. Phys.*, Vol. 325, 2006, pp. 299-312.

[18] M. Renardy, On the use of Laplace transform inversion for reconstruction of relaxation spectra, *J. Non-Newtonian Fluid Mech.*, Vol. 154, 2008, pp. 47-51.

[19] V. Shtrauss, Functional conversion of signals in the study of relaxation phenomena, *Signal Processing*, Vol. 45, 1995, pp. 293-312.

[20] V. Shtrauss, Unified approach and technique to performance of Mellin convolution and related integral transform in relaxation experiments, *Meccanica*, Vol. 32, 1997, pp. 251-258.

[21] V. Shtrauss, Signal processing in relaxation experiments, *Mech. Comp. Mat.* Vol. 38, 2002, pp. 73–88.

[22] V. Shtrauss, Digital signal processing for relaxation data conversion, *J. Non-Crystal. Solids*, Vol. 351, 2005, pp. 2911-2916.

[23] V. Shtrauss, Spectrum analysis and synthesis of relaxation signals, *Signal Processing*, Vol. 63, 1997, pp. 107-119.

[24] V. Shtrauss, FIR Kramers-Kronig transformers for relaxation data conversion, *Signal Processing*, Vol. 86, 2006, pp. 2887-2900.

[25] V. Shtrauss, Determination of relaxation and retardation spectrum by inverse functional filtering, *J. Non-Newtonian Fluid Mech.*, Vol. 165, 2010, pp. 453-465.

[26] V. Shtrauss, Digital estimators of relaxation spectra, *J. Non-Crystal. Solids*, Vol. 353, 2007, pp. 4581-4585.

[27] A.V. Oppenheim, R.V. Schafer, *Discrete-Time Signal Processing*, Sec. Ed., Prentice-Hall International, 1999.

[28] J. Bertrand, P. Bertrand, J-P. Ovarlez, Chapter 12 „The Mellin Transform", in *The Transform and Applications Handbook*, Ed. A.D. Poularikas, CRC Press inc., 1995.

[29] H.W. Engl, M. Hanke, A. Neubauer, *Regularization of Inverse Problems*, Kluwer, Dordrecht, 1996.

[30] V. Shtrauss, Inverse filters for decomposition of multi-exponential and related signals, *Proc. 7th WSEAS International Conference on Systems Theory and Scientific Computation (ISTASC'07)*, Athens, Greece, August 24-26, 2007, pp. 135-140.

[31] V. Shtrauss, Decomposition of multi-exponential and related signals – Functional filtering approach, *WSEAS Transactions on Signal Processing*, Vol. 4, 2008, pp. 44-52.

[32] V. Shtrauss, Sampling and algorithm design for relaxation data conversion, *WSEAS Transactions on Signal Processing*, Vol. 2, 2006, pp. 984-990.

[33] V. Shtrauss, Sampling in relaxation data conversion, *Proc. 10th WSEAS International Conference on SYSTEMS*, Vouliagmeni, Athens, Greece, July 10-12, 2006, pp. 37-42.

[34] H.M. Nussenzveig, *Causality and Dispersion Relations*; Academic Press, 1972.

[35] K.S. Cole, R.H. Cole, Dispersion and absorption in dielectric. Alternating current characteristics, *J. Chem. Phys.*, Vol. 9, 1941, pp. 341-351.